Evaluation of Corrosion Inhibition Efficiency of Poly(1,4-trans Myrcene-co-Styrene) Copolymer on Carbon Steel in a Hydrochloric Acid Solution

H. Haddouchy[1]*, S. Loughmari[2], M. Oukbab[3], Y. Tahiri[3], M. Oubaouz[3], F. Z. Hamid[1], A. Smaini[3], A. El Bouadili[2], M. Visseaux[4], A. Chtaini[3] and S. E. El Qouatli[1]

[1] *Physical Chemistry Environment and Material, Faculty of Sciences and Technologies, Moulay Ismail University, Errachidia, Morocco*
[2] *Laboratory of Industrial Engineering and Surface Engineering, Applied Chemistry and Environmental Sciences Team, Faculty of Sciences and Technology, Sultan Moulay Slimane University, Beni Mellal, Morocco*
[3] *Electrochemistry and Molecular Inorganic Materials Team, Faculty of Sciences and Technology, Sultan Moulay Slimane University*
[4] *CNRS, Central Lille University, Artois, UCCS, Catalysis and Solid Chemistry Unit, Lille, France*
*Corresponding author: ha.haddouchy@gmail.com

Received 21/06/2024; accepted 10/12/2024
https://doi.org/10.4152/pea.2026440601

Abstract
The long-standing history of low corrosion resistance in E316 CS poses a persistent challenge for its industrial applications. Green CI are among the most widely adopted and cost-effective methods to protect metals and alloys against corrosion. In this study, a novel approach involving controlled block polymerization of myrcene, a biobased isoprene dimer, with styrene, using a $Nd(BH_4)_3(THF)_3$/BEM-based catalytic system, resulted in the synthesis of poly(1,4-trans myrcene-co-styrene) - PMy- copolymer. This transparent and adhesive copolymer was developed as CI agent. Experiments were conducted using WL method and electrochemical techniques, at various polymer Ct and IT. According to the results obtained from WL and electrochemical analyses, increased IE(%) was observed using a polymer Ct of V3, corresponding to 1,5 g/L, suggesting higher corrosion IE(%) properties. Electrochemical analyses revealed that PMy exhibited a uniform CI effect, with a cathodic predominance. Additionally, R_{ct} of CS electrode in an untreated solution increased from 71.25 to 668.3 Ω cm^{-2}, in a solution with PMy, after 24 h of IT.

Keywords: CI; E316 CS; HCl solution; PMy.

Introduction•

Metallic materials, especially Fe and its alloys, play a crucial role in construction and various related industries [1]. However, Fe alloys are highly susceptible to

• The abbreviations list is in pages 404-405.

corrosion when exposed to humid environments, immersed in fresh or saltwater, implanted in soil, or subjected to other aggressive solutions [2, 3]. Among these corrosive environments, acidic solutions, notably, HCl, induce significant corrosion and degradation of industrial equipment. The use of inhibitors is one of the most practical methods to prevent substantial damage to metals, especially in acidic environments. HCl solutions are widely employed in processes such as pickling, cleaning and descaling of stainless steel [4, 5]. Various compounds, including plant extracts rich in active molecules [6, 7] and organic molecules, have been investigated so as to reduce CR of materials [8, 9].

The presence of heteroatoms, aromatic rings, conjugated bonds, as well as nitrogen and oxygen atoms, enhances these processes [8-11], slowing down metal corrosion in different ways, depending on environmental properties and conditions. In the continuation of our research on the development of organic compounds as acid inhibitors, we have selected inhibitors of the polymer type PMy. These compounds structurally consist of variable arrangements of β-myrcene, natural dimer of isoprene units (C5) and styrene. Natural polymer elastomers, obtained from rubber trees, have been used for centuries in various applications such as latex gloves, vehicle tires and children's toys [12]. Myrcene, a volatile aromatic hydrocarbon present in plants like hops, citronella, cannabis and laurel leaves, is a versatile monomer.

Coordination polymerization, a robust method, enables polymerization of various monomers, including dienes such as isoprene, myrcene and styrene [13-15]. To our knowledge, no publication has addressed the performance of PMy copolymer for protecting CS against corrosion in 1 M HCl. Tests involving WL, over different IT time, at several polymer Ct, were conducted, along with electrochemical techniques, such as PDP and EIS, under various experimental conditions, to assess the effect of PMy addition on its IE(%) in HCl.

Materials and methods

Synthesis of inhibitor

All procedures were carried out under dry argon, using either a glove box or Schlenk techniques. Toluene was purified using alumina columns (Mbraun SPS), distilled from trap to trap, over sodium/benzophenone ketyl, and then stored on molecular sieves (3A), inside the glove box. β-myrcene and styrene, from Aldrich, were dehydrated using calcium hydride, distilled once over molecular sieves, and once again just before use. BEM (20 wt% in heptane from Texas Alkyls) was used as-received. $Nd(BH_4)_3(THF)_3$ was synthesized following procedures outlined in literature [7].

NMR spectra of both PMy copolymers were acquired using a Bruker Advance 300 spectrometer, at 300 K, with $C_2D_2Cl_4$ serving as solvent for ^1H experiments. Quantitative ^{13}C NMR analysis was performed in $CDCl_3$, utilizing zgig sequence.

SEC was performed in THF, at 40 ºC, with a flow rate of 1 mL/min. This process involved Waters SIS HPLC-pump, Waters 410 refractometer and Waters Styragel column (HR2, HR3, HR4 and HR5E). Polystyrene standards were employed for calibration.

Materials and solutions

Chemical composition (expressed as weight percentage) of C steel samples used in this study is as follows: < 0,08 Mn, < 0,9 Si, < 0,9 S, < 0,03 P and remaining Fe. CS samples were initially polished with abrasive paper ranging from 400 to 1600 grit, followed by rinsing with distilled water and air drying. A 1 cm^2 exposed surface was brought into contact with aggressive solutions. The test solution (1.0 mol/L HCl) was prepared by diluting 37% analytical-grade HCl (Sigma Aldrich, France) with distilled water. Polymer volumes were measured using a micropipette.

Electrochemical measurements

Electrochemical experiments were conducted using a VoltaLab potentiostat (model PGSTAT 100, Eco Chemie BV, Utrecht, Netherlands), controlled by data processing software for general electrochemical systems (VoltaLab Master 4 software), for general purposes. All electrochemical experiments were carried out in a compartment of a standard three-electrode system. SCE and Pt were employed as RE and CE, respectively. The electrodes E were standardized with respect to RE. WE was composed of CS (E316).

Result and discussion

WL measurements

CS samples were prepared following ASTM G1-03 [16] procedures for WL tests. After being prepared and weighed, CS samples were suspended and immersed in a 1.0 M HCl solution with varying Ct from PMy. Subsequently, samples were submerged in HCl for 24, 48 and 72 h, at a temperature of 298 K. Afterwards, the samples were removed, rinsed with distilled water and then reweighed. Obtained average WL values (ΔW) were used to calculate CR (mm/year) and IE(%), using Eqs. (1-2) [16].

$$CR = \frac{8.67 * 10000 * \Delta w}{\rho A t} \quad (1)$$

$$\eta w\ \% = \frac{CR - CR}{CR} * 100 \quad (2)$$

where A is CS surface area in 1 cm^2, t is IT in h, p is alloy density in g/cm^{-1} and K is a conversion parameter representing CR, in different units. CR and CRi refer to CR without and with inhibitor, respectively.

The transparent polymer yielded up to 60 %, which demonstrates a monomodal molecular weight distribution, as shown in Fig. 1. PDI (MW) was 1.46.

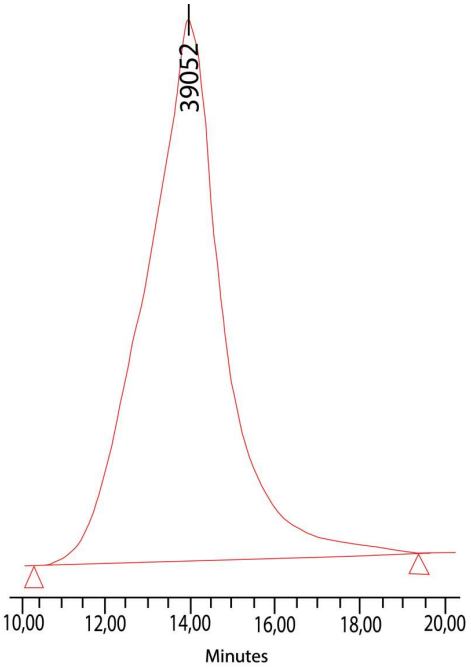

Figure 1: Chromatogram of PMy.

PDI value below 2 indicates a single-site nature of copolymerization, suggesting homopolymers absence. PMy's NMR spectra (^{1}H and ^{13}C) revealed that around 10 % styrene was incorporated into the polymer (Fig. 2).

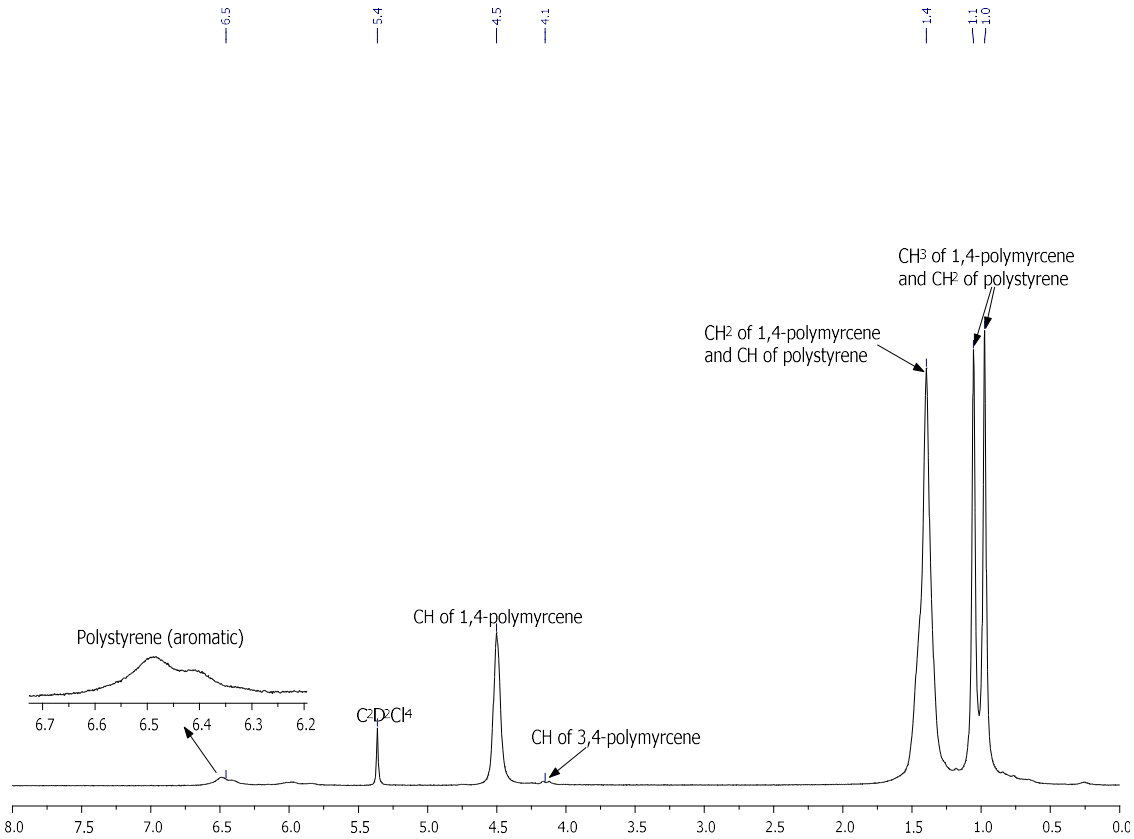

Figure 2: ^{1}H NMR spectrum (300 MHz, $C_2D_2Cl_4$) of PMy.

^{1}H NMR spectrum of the copolymer display signals representing the existence of PMy within the copolymer structure. Additionally, the spectrum exhibit signals corresponding to the protons of the styrene aromatic units present in the copolymer, alongside other supplementary signals.
From the analysis of ^{13}C NMR (Fig. 3), C signals corresponding to the myrcene backbone have been differentiated based on their adjacent motifs.

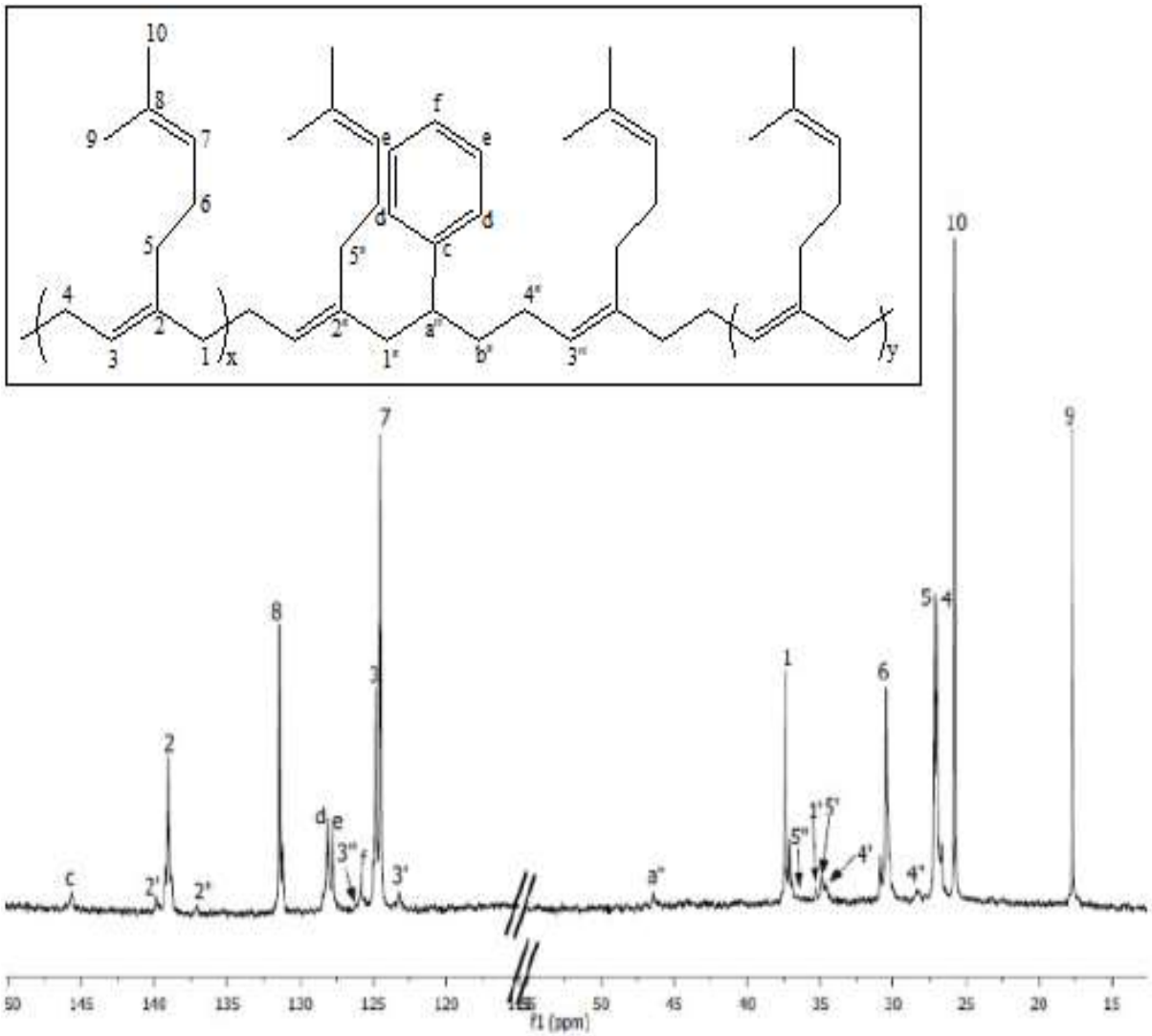

Figure 3: ^{13}C NMR spectrum (75 MHz, $CDCl_3$) of PMy.

The most significant signal was attributed to PMy. As this acyclic monoterpene was predominantly present within the copolymer (89.28 %), myrcene-myrcene sequences were expected to be the most abundant. Consequently, this determined the co-polymer's microstructure (Fig. 4). Furthermore, the substantial quantity of styrene present in the reactive environment did not impact the reaction's stereoselectivity. Even with the incorporation of up to 10 % styrene under the given experimental conditions, the copolymer backbone exhibited 90.8 % 1,4-trans microstructure.

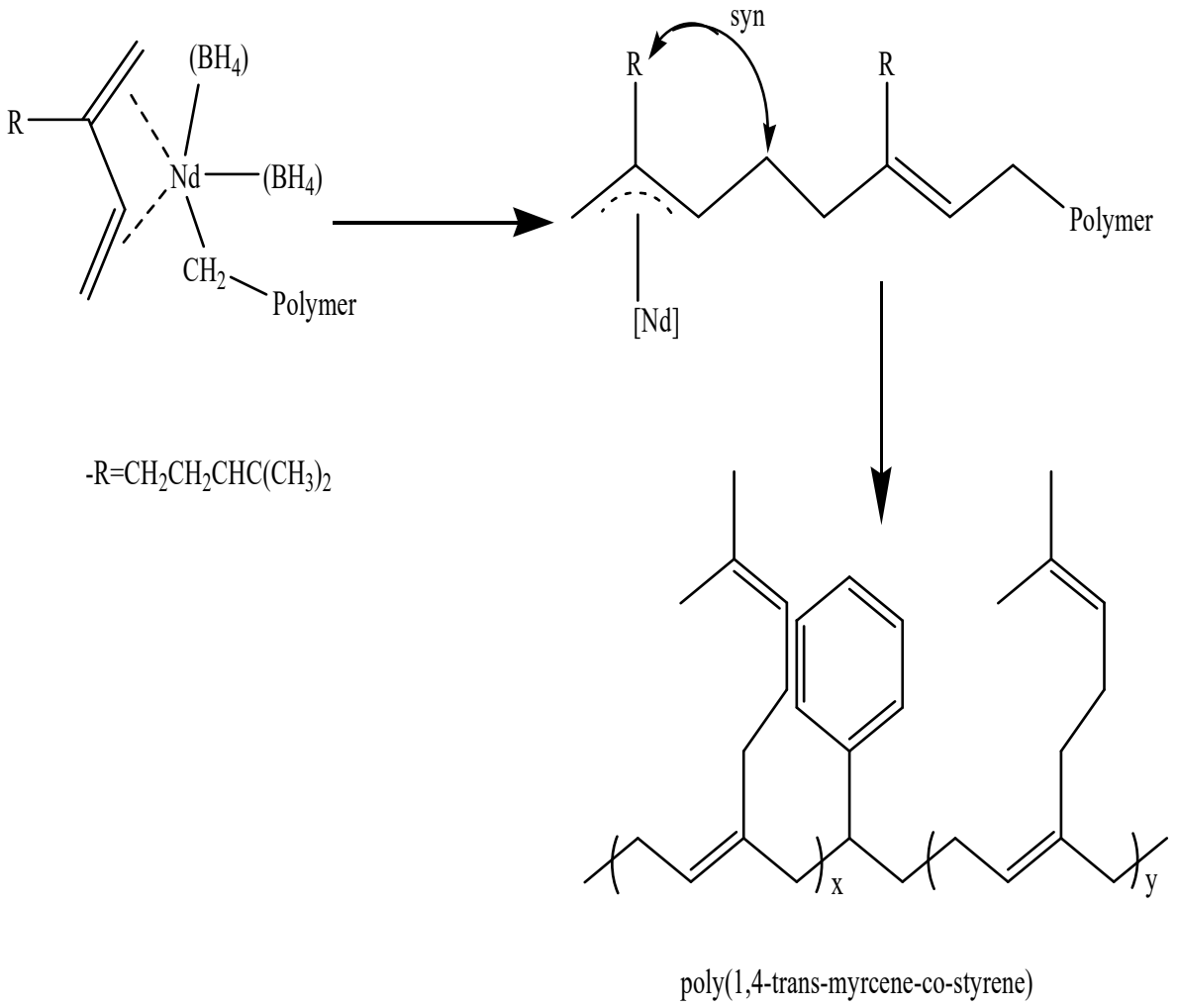

Figure 4: Microstructure of PMy.

WL measurements

WL technique has proven to be an effective non-electrochemical method for assessing the CR of metals at different inhibitor Ct in a 1 M HCl solution, and for varying IT.

The results demonstrate that CS samples underwent significant corrosion in the inhibited HCl solution, but, with inhibitors, CR was significantly reduced.

Data presented in Table 1 and Fig. 5 indicate that the polymer addition led to a decrease in CR, and a corresponding increase in IE(%), especially noteworthy in V3 polymer (83.1596 %) presence. This observation can be explained by the polymer's adsorption onto the CS surface, which blocked reaction sites.

Table 1: Impact of the addition of polymer compounds to CS on its CR over a 72 h IT.

Ct of polymer	CR (mm/year)	IE(%)
Blank	1,4299	----------
V_1-polymer	0,9889	30,8413
V_2- polymer	0,7074	50,5052
V_3- polymer	0,2408	83,1596

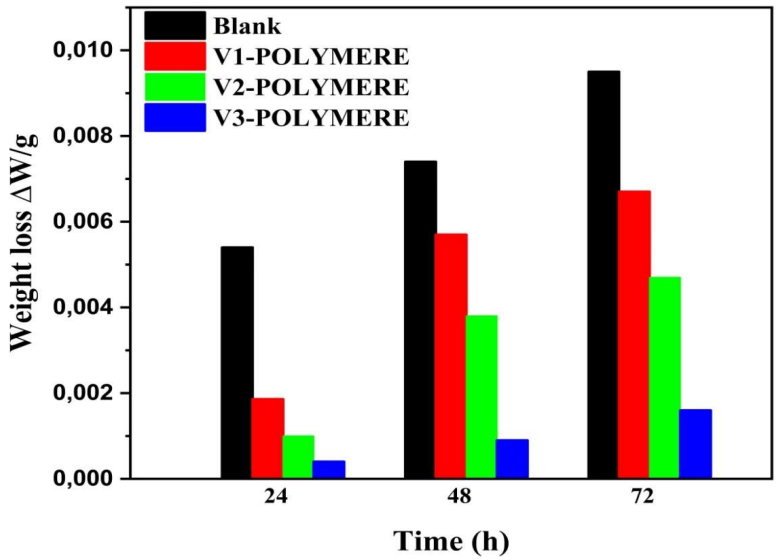

Figure 5: WL variation in relation to the IT of CS in a 1 M HCl solution with v_1, v_2 and v_3 polymers.

IE(%) evaluation, conducted using WL method, revealed satisfactory agreement between CR measurements and experimental observations.

PDP curves

In order to better understand CS (E 316) behavior in a 1 M HCl solution, cathodic and anodic polarization curves were calculated without and with PMy (Fig. 6).

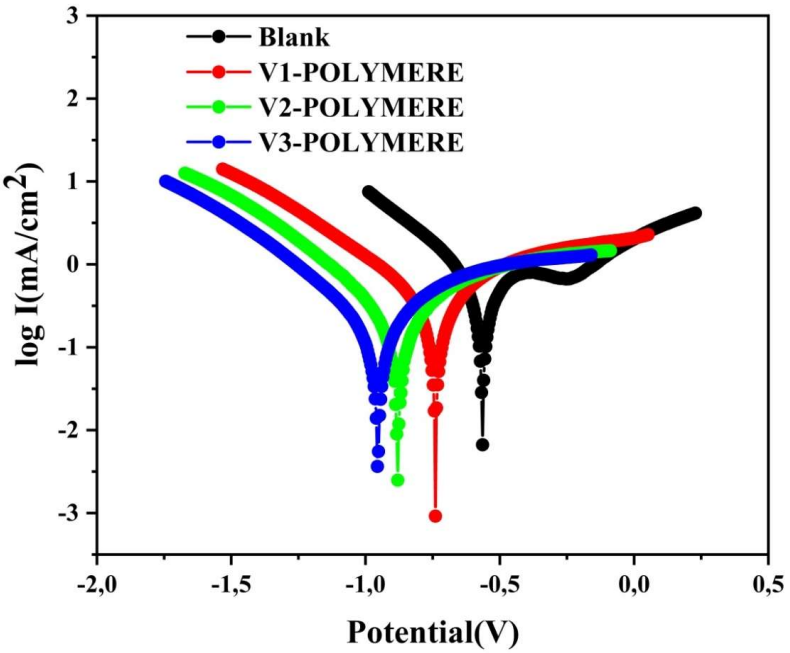

Figure 6: PDP curves for CS with and without various polymer Ct in 1 mol/L^{-1} HCl.

The analysis of this figure reveals that the polymer addition to the HCl solution led to a reduction in i_{corr} compared to the blank solution, as well as a significant shift in E_{corr}

towards cathodic direction. This trend was directly proportional to the added polymer Ct.

Furthermore, a linear region was observed in the cathodic domain, suggesting a good agreement of Tafel line in this region. A slight increase was noticed around -0.2 V/SCE, for the polymer-free solution, typically associated with hydrogen desorption, known as desorption E.

The reductions in i_{corr}, E_{corr}, β_c and β_a, as well as IE(%) for different Ct of the polymer, are listed in Table (2). IE(%) was calculated according to Eq. (3):

$$IE\ \% = \frac{Icorr - Icorr(inh)}{Icorr} * 100 \qquad (3)$$

where i_{corr} and $i_{corr(inh)}$ represent i_{corr} of non-inhibited and inhibited CS, respectively, determined by extrapolating cathodic Tafel lines or E_{corr}.

By analyzing cathodic and anodic PDP curves in Fig. 6, and electrochemical parameters in Table 2, it was concluded that the studied polymer significantly inhibited both corrosion processes.

In conclusion, PMy copolymer acts as a highly effective CI, significantly enhancing the corrosion resistance of CS in a 1 M HCl solution. The polymer forms a protective barrier on the steel surface, reducing metal dissolution (anodic reaction) and hydrogen evolution (cathodic reaction). IE(%) increases with the polymer Ct, suggesting that the protective effect can be optimized with higher polymer doses. This study demonstrates the polymer's potential for industrial applications where CS is subjected to harsh acidic environments. Future research could explore the long-term stability of the polymer's protective layer and its behavior in more complex or dynamic corrosive conditions.

Table 2: PDP parameters for corrosion of CS in 1.0 mol/L-1 HCl without and with different polymer Ct.

Polymer	E_{corr} (mV/SEC)	I_{corr} ($\mu A/cm^{-2}$)	βa (mV)	βc (mV)	IE(%)
Blank	-564,1	688,3	1019,8	-412,1	--------
V_1-polymer	-739,8	415,1	685,5	-495,5	39,69
V_2- polymer	-879,7	345,8	873,6	-474,7	49,76
V_3- polymer	-954,7	233,8	628,1	-453,5	66,03

On the other hand, the effect of the contact between VS plate and polymer was examined for IT of 4, 12 and 24 h, followed by characterization in HCl. Fig. 7 presents recorded PDP curves. It is observed that an increase in the contact time was associated with a decrease in i_{corr} and a shift in E_{corr} towards the cathodic region.

Analyzing cathodic and anodic PDP curves from Fig. 7, along with electrochemical parameters in Table 3, one can conclude that the studied polymer significantly inhibited the corrosion process of CS in HCl. A high IE(%) of 82.96, at 24 h, attested to the polymer's excellent performance, due to its adsorption onto the electrode surface. This formed a film that acted as a protective barrier against corrosive species,

thereby reducing the attacked CS surface. Variations in IE(%) can be explained by the effects of IT and Ct, facilitated by adsorption.

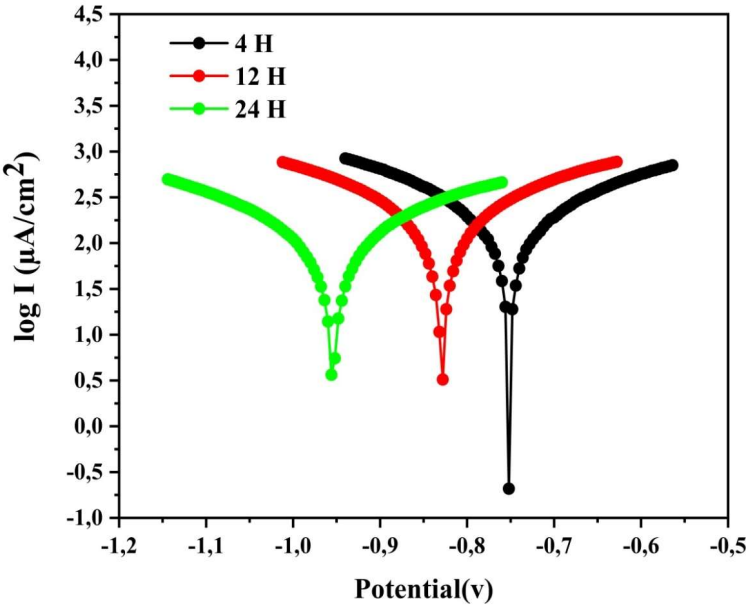

Figure 7: PDP curves for CS immersed in polymer at different IT, followed by immersion in a 1 mol/L^{-1} HCl solution.

Table 3: PDP parameters for corrosion of CS in 1.0 mol/L^{-1} HCl immersed in the polymer at different IT.

IT	E_{corr} mV (SCE)	I_{corr} (µA/cm^{-2})	β_a (mV)	β_c (mV)	IE(%)
Blank	-564,1	688,3	1019,8	-412,1	----------
4 h	-751,2	224,999	357	-327,3	67,31
12 h	-828,8	199,9246	358	-333,7	70,95
24 h	-954,4	117,34	311	-299,8	82,96

EIS measurements

EIS spectra obtained for different Ct of polymer, and E_{corr}, are depicted in Fig. 8. EIS is a non-destructive technique useful for characterizing CI properties. These measurements were conducted over a wide frequency range and at room temperature.

Upon examining EIS, one notes that it consists of a small diameter loop. Following the addition of various Ct of polymer to HCl solutions, an increase was seen. This was due to the polymer adsorption on the CS surface, replacing water molecules at steel/HCl interface.

Electrochemical parameters obtained from fitting EIS diagrams are listed in Table 4. Analysis of data in this table reveals that the polymer addition led to a significant increase in R_p, from 71.25 (blank) to 629.9 Ω/cm^{-2}, in V_3-polymer presence. This rise in R_p was due to the polymer adsorption onto the CS surface, forming a protective film against corrosion. It can also be concluded that the polymer adhesion to the CS surface may have altered the double electric layer, thereby reducing HCl solution attack, and enhancing IE(%).

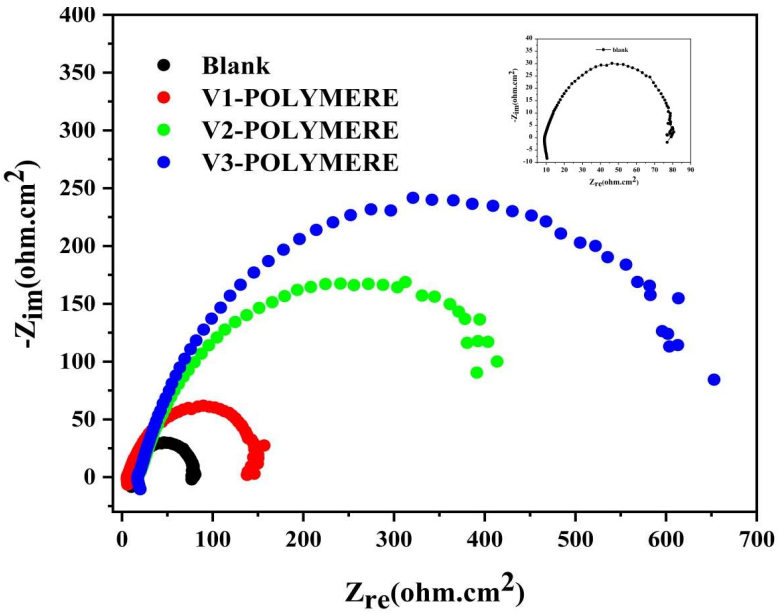

Figure 8: EIS graphs of CS without and with various polymer Ct in a 1 mol L^{-1} HCl solution.

Table 4: EIS parameters of steel in 1 M HCl without and with the polymer, at different Ct.

	Diameter (Ω/cm^{-2})	Correlation	R_1 (Ω/cm^2)	R_2 (Ω/cm^2)	R_1 - R_2
Blank	71,25	0,969	9,878	70,39	60.512
V_1-polymer	148,7	0,936	7,120	146,3	139.18
V_2- polymer	527	0,973	18,30	492,7	474.4
V_3- polymer	699,9	0,8	21,62	674,7	653.08

Bode plots presented in Fig. 9 revealed a consistent peak in both inhibited and uninhibited samples, confirming the validity of the equivalent circuit used to obtain EIS results.

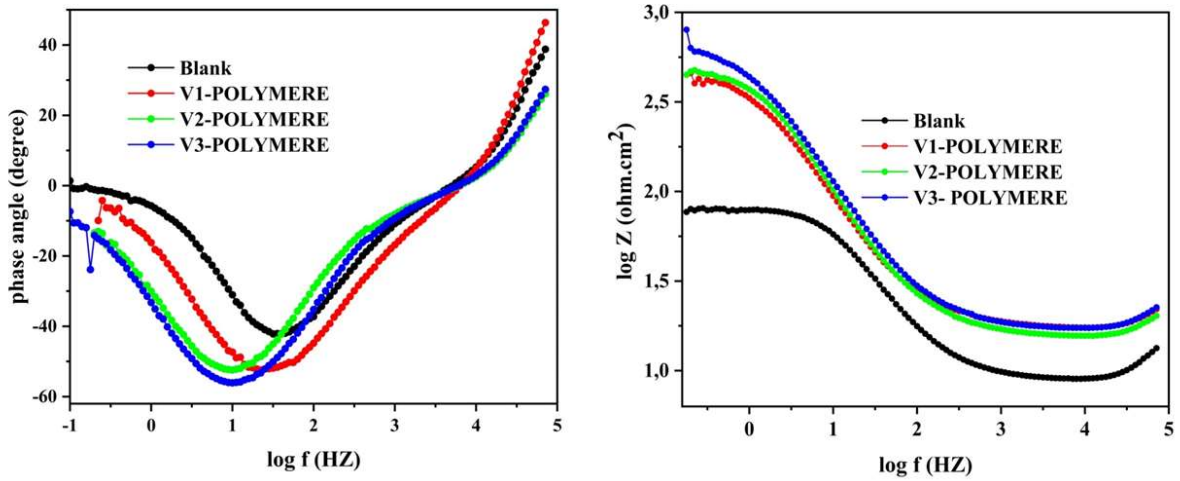

Figure 9: Bode plots for E316 steel in HCL without and with the polymer, at different Ct.

Furthermore, Bode plots indicate a single maximum phase, suggesting that R_{ct} at the interface between CS and solution reacted to the electrochemical process.

Additionally, as the polymer Ct increased, phase angle values rose to 55 compared to the blank solution, and a significant increase in impedance was observed.
This indicates an improvement in IE(%), due to the polymer's adsorption onto the steel surface. More specifically, the polymer can react with hydrogen ions in the acid to form non-corrosive products, which create a protective layer on the CS surface, thereby preventing them from reaching the metal surface. Fig. 10 represents equivalent circuit.

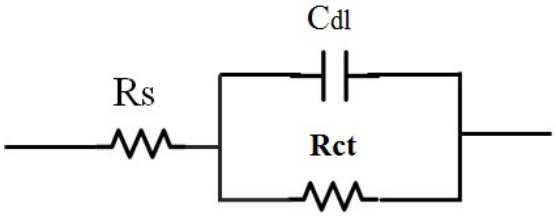

Figure 10: Equivalent circuit model used for EIS fitting.

Effect of IT

The evolution of EIS diagrams for CS, or E_{corr}, in the presence of V_3 polymer, as a function of IT, is depicted in Fig. 11, along with the results of the Ct effect. The loop size increased with prolonged IT, confirming excellent corrosion protection properties. Additionally, it can be seen that both phase angle and impedance proportionally increased with IT. This trend can be explained by the significant increase in the film resistance over IT.

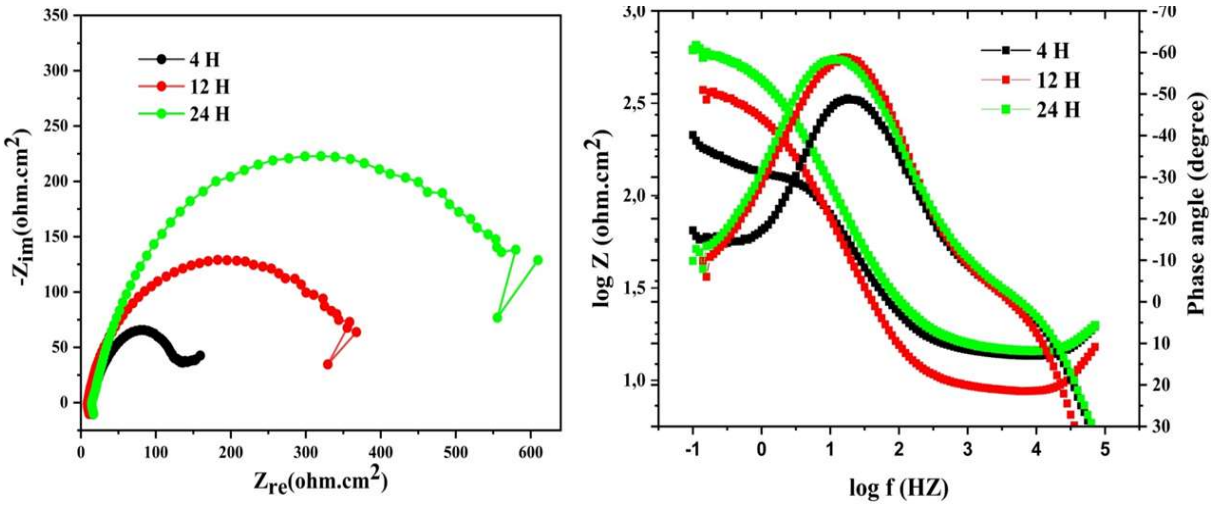

Figure 11: EIS diagrams of effect of IT on CS with V_3 polymer in a 1 mol/L^{-1} HCl solution.

With extended IT, the inhibitor film on the steel surface gained greater strength, thereby enhancing its corrosion resistance. Determined impedance parameters are listed in Table 5. Results reveal a significant increase in the resistance of the formed film, with IT, indicating the formation of a highly protective barrier.

These observations reflect a marked improvement in the CI effect of the polymer with prolonged IT. This suggests that, with longer IT, the adsorption of polymer components onto the CS surface was stronger.

Table 5: EIS parameters of CS immersed in the polymer, in 1 M HCl, at different IT.

IT	Diameter (Ω/cm^{-2})	Correlation	R_1 (Ω/cm^2)	R_2 (Ω/cm^2)	R_1 - R_2
4 h	164,3	0,8	15,3	160,6	145,3
12 h	397,9	0,979	9,005	375,5	366,495
24 h	668,3	0,971	14,84	634,7	619,86

Conclusions

In this study, a new application of PMy copolymer was prepared and investigated to protect E316 CS in a 1 mol/L^{-1} HCl solution. An experimental approach was employed to assess the IE(%) of the CI.

The copolymer's IE(%) proportionally increased with Ct, reaching a maximum value of 82.96. PDP curves indicated that PMy acted as a good CI, predominantly influencing cathodic side. EIS measurements revealed an increase in R_p values with higher copolymer's Ct and IT. This notable CI resulted from PMy's adsorption onto the CS surface, forming a protective film that hindered HCl attack on the CS.

Studies on PMy copolymer are globally becoming a highly attractive area, highlighting the exploration of alternative recycling pathways.

Acknowledgements

We sincerely express our gratitude to the Molecular Electrochemistry and Inorganic Materials team at the Faculty of Science and Technology, Beni Mellal. Additionally, we acknowledge the Laboratory of Chemistry Physics, Environment and Materials, at Faculty of Sciences and Techniques, Errachidia. Their unwavering support and collaboration have been invaluable to the success of this research project.

Authors' contributions

H. Haddouchy: contributed to conceptualization, experimental investigation, data analysis; prepared the original version, revising and editing. **S. Loughmari**: contributed to conceptualization. **M. Oukbab**: contributed to conceptualization. **Y. Tahiri** and **M. Oubaouz**: conducted experimental studies. **F. Z. Hamid**: directed experimental research. **A. Smaini**: conducted experimental study. **A. El Bouadili** and **M. Visseaux**: in charge of data analysis. **A. Chtaini**: contributed to data analysis and methodology; provided supervision. **S. E. El Qouatli**: conceptualization; methodology; preparation of the original revision and editing.

Abbreviations

β_a: anodic Tafel slope

β_c: cathodic Tafel slope
BEM: n-butylethyl magnesium
$C_2D_2Cl_4$: 1,1,2,2-Tetrachloroethane-d2
$CDCl_3$: chloroform-d1
CE: counter electrode
CI: corrosion inhibitor/inhibition
CPE: carbon paste electrode
CR: corrosion rate
CS: carbon steel
Ct: concentration
DSC: differential scanning calorimetry
E: potential
E_{corr}: corrosion potential
EIS: electrochemical impedance spectroscopy
Fe: iron
HCl: hydrochloric acid
i_{corr}: corrosion current density
IE(%): inhibition efficiency
IT: immersion time
Mn: manganese
MW: average molecular weight
$Nd(BH_4)_3(THF)_3$: neodymium trisborohydride
NMR: nuclear magnetic resonance
P: phosphorus
PDI: polydispersity index
PDP: potentiodynamic polarization
PMy: poly(1,4-trans myrcene-co-styrene)
R_{ct}: charge transfer resistance
RE: reference electrode
R_p: polarization resistance
S: sulfur
SCE: saturated calomel electrode
SEC: size exclusion chromatography
THF: tetrahydrofuran
WE: working electrode
WL: weight loss

References

1. Cao Z, Tang Y, Cang H et al. Novel benzimidazole derivatives as corrosion inhibitors of mild steel in the acidic media. Part II: Theoretical studies. Corros Sci. 2014;83:292-298. https://doi.org/10.1016/j.corsci.2014.02.025

2. Chebabe D, Abbout S, Damej M et al. Electrochemical and Theoretical Study of Corrosion Inhibition on Carbon Steel in 1M HCl Medium by 1,10-Bis(4-Amino-3-Methyl-1,2,4-Triazole-5-Thioyl)Decan. Analyt Prev. 2020;20:1673. https://doi.org/10.1007/s11668-020-00974-y
3. Bouhlal F, Labjar N, Abdoun F et al. Chemical and electrochemical studies of the inhibition performance of hydro-alcoholic extract of used coffee grounds (HECG) for the corrosion of C38 steel in 1 M hydrochloric acid. Egyp J Petr. 2019;29:45-52. https://doi.org/10.1016/j.ejpe.2019.10.003
4. Trabanelli G. 1991 Whitney Award Lecture: Inhibitors—An Old Remedy for a New Challenge. Corrosion. 1991;(47)6:410-419. https://doi.org/10.5006/1.3585271
5. Haque J, Ansari KR, Srivastava V et al. Pyrimidine derivatives as novel acidizing corrosion inhibitors for N80 steel useful for petroleum industry: A combined experimental and theoretical approach. J Ind Eng Chem. 2017;49:176-188. https://doi.org/10.1016/j.jiec.2017.01.025
6. Hammouch H, Dermaj A, Chebabe D et al. Opuntia Ficus *Indica* Seed Oil: Characterization and Application in Corrosion Inhibition of Carbon Steel in Acid Medium. Analyt Bioanalyt Electrochem. 2013;5(2):236-254.
7. Damej M, Zouarhi M, Doubi M et al. Study of the protective effect of green inhibitor extracted from seeds oil of *Cannabis sativa L.* against corrosion of brass 60Cu–40Zn in seawater medium. Int J Corros Scale Inhib. 2020;(9)4:1564-1579. https://doi.org/10.17675/2305-6894-2020-9-4-24
8. Raicheva SN, Aleksiev BV, Sokolova EI. The effect of the chemical structure of some nitrogen- and sulphur-containing organic compounds on their corrosion inhibiting action. Corros Sci. 1993;34:343-350. https://doi.org/10.1016/0010-938X(93)90011-5
9. Bouayed M, Rabaa H, Schiri A et al. Experimental and theoretical study of organic corrosion inhibitors on iron in acidic medium. Corros Sci. 1999;(41)3:501-517. https://doi.org/10.1016/S0010-938X(98)00133-4
10. Chellouli M, Chebabe D, Dermaj A et al. Corrosion inhibition of iron in acidic solution by a green formulation derived from *Nigella sativa L*. Electrochim Acta. 2016;204:50-59. https://doi.org/10.1016/j.electacta.2016.04.015
11. Akounach Z, Al Maofari A, El Yadini A et al. Inhibition of Mild Steel Corrosion in 1.0 M HCl by Water, Hexane and Ethanol Extracts of *Pimpinella Anisum* Plant Analytic Analy Bioanaly Electrochem. 2018;10(11):1506-1524.
12. Dinsmore RP. Synthetic rubber and method of making it. U. S. Patent US1732795A, 1927.
13. Terrier M, Visseaux M, Chenal T et al. Controlled trans-stereospecific polymerization of isoprene with lanthanide(III) borohydride/dialkylmagnesium systems: The improvement of the activity and selectivity, kinetic studies, and mechanistic aspects. J Polym Sci, Part A. 2007;(45)12:2400-2409. https://doi.org/10.1002/pola.22002

14. Loughmari S, Hafid A, Bouazza A et al. Highly stereoselective coordination polymerization of β-myrcene from a lanthanide-based catalyst: Access to bio-sourced elastomers. J Polym Sci, Part A: Polym Chem. 2012;(50)14:2898-2905. https://doi.org/10.1002/pola.26069
15. Zinck P, Visseaux M, Mortreux A. Borohydrido Rare Earth Complexes as Precatalysts for the Polymerisation of Styrene. Anorg Z Allg Chem. 2006;(632) 12-13: 1943-1944. https://doi.org/10.1002/zaac.200600143
16. Hsissou R, Abbout S, Seghiri R et al. Evaluation of corrosion inhibition performance of phosphorus polymer for carbon steel in [1 M] HCl: Computational studies (DFT, MC and MD simulations). J Mater Res Technol. 2020;(9)3:2691-2703. https://doi.org/10.1016/j.jmrt.2020.01.002